Electronic Supplementary Material (ESI) for Journal of Materials Chemistry C.

Supporting Information

Fast fabrication of double-layer printed circuits based on bismuth-based low-melting alloy beads

Pengju Zhang, Yang Yu, Bowei Chen, Wei Wang, Zhiqiang Cao, Sijian Wei, Wei Rao, Qian Wang**

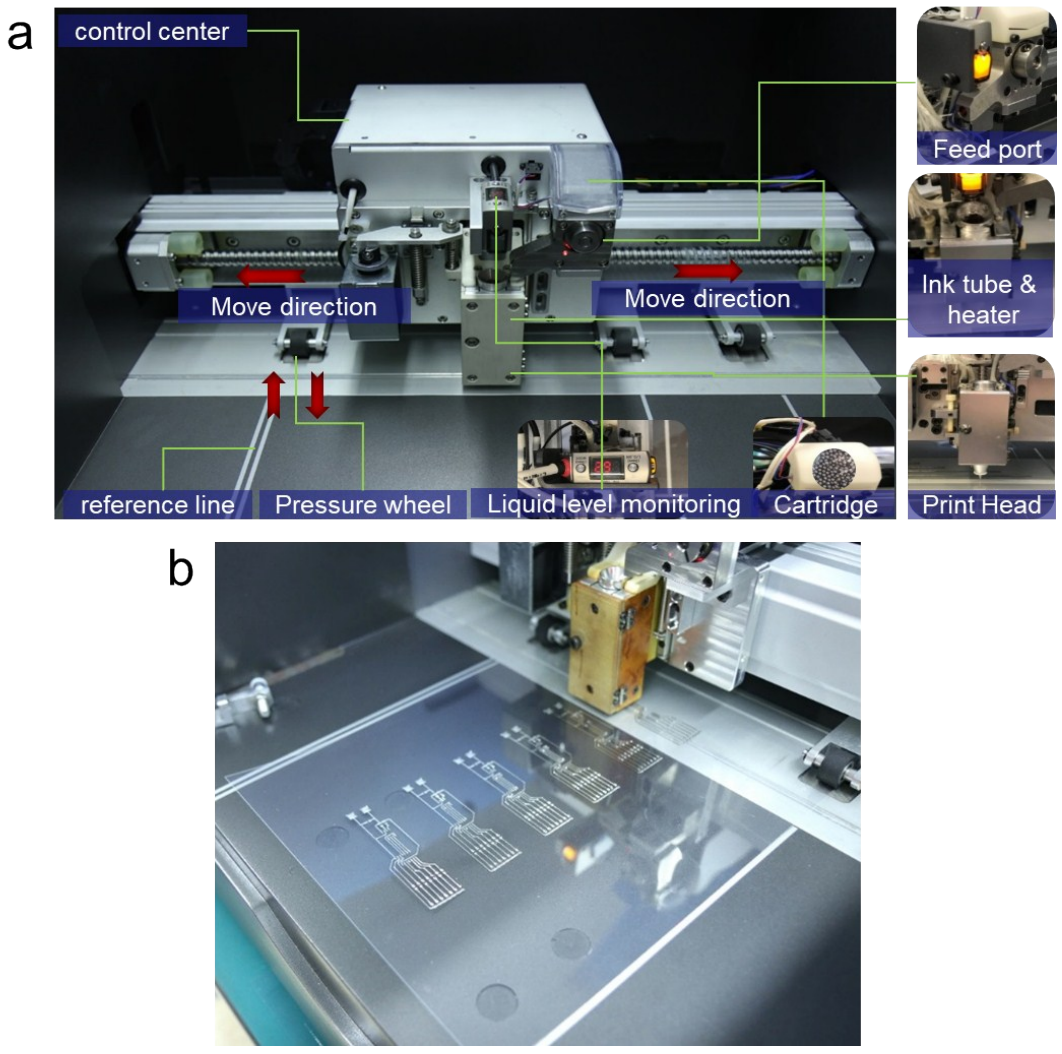

Figure S1. (a) The low-melting metal printing device. The entire printing device has an intelligent control center which is responsible for controlling the corresponding components to print the input circuit by connecting with a computer, and also a cartridge to store raw materials, movement component to transfer materials, ink tube with a heater and a print head to heat the raw material and write it down. The spiral guide can control the moving direction of the print head to realize the free movement of two-dimensional planes. (b) Process of printing circuit.

As shown in Figure S2, the BiInSn lines without encapsulation layer can still keep undamaged after rubbing at room temperature. This is one of the advantages compared with gallium-based liquid metal. Of course, when the printed circuits are applied in an environment that is higher than the melting point of the Bi-based alloy, the necessary packaging procedure is still required. In fact, in the field of electronic circuit applications, if the electronic circuit is used for a long time under a higher temperature environment, not only the conductive lines, but most components in the electronic circuit would greatly reduce their life and reliability.[1-3].The working temperature of general integrated circuits is divided into commercial grade (C) (0 ~ 70°C), industrial grade (I) (-40 ~ 85°C), and military grade (M) (-55 ~ 125°C or wider).[4.5] Bi-based alloy in this study with melting point of 79.6 °C can fully meet the use requirements of commercial-grade integrated circuits.

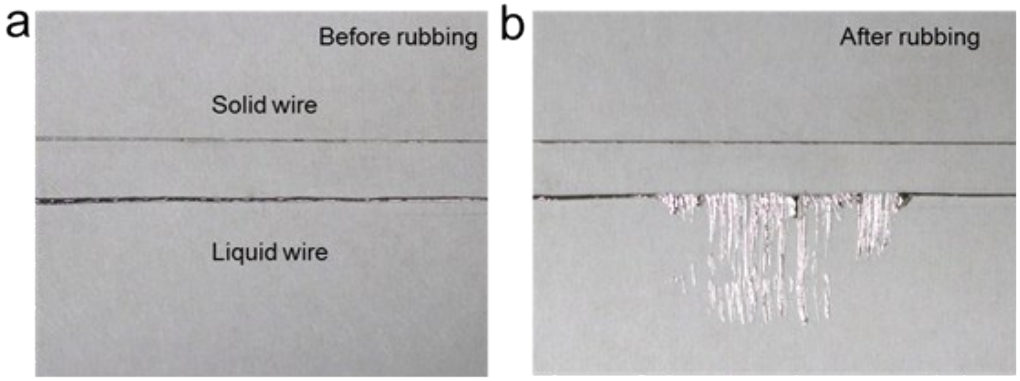

Figure S2. Differences between printed solidified wire with printed liquid wire without a package. (a) Before rubbing. (b) After rubbing.

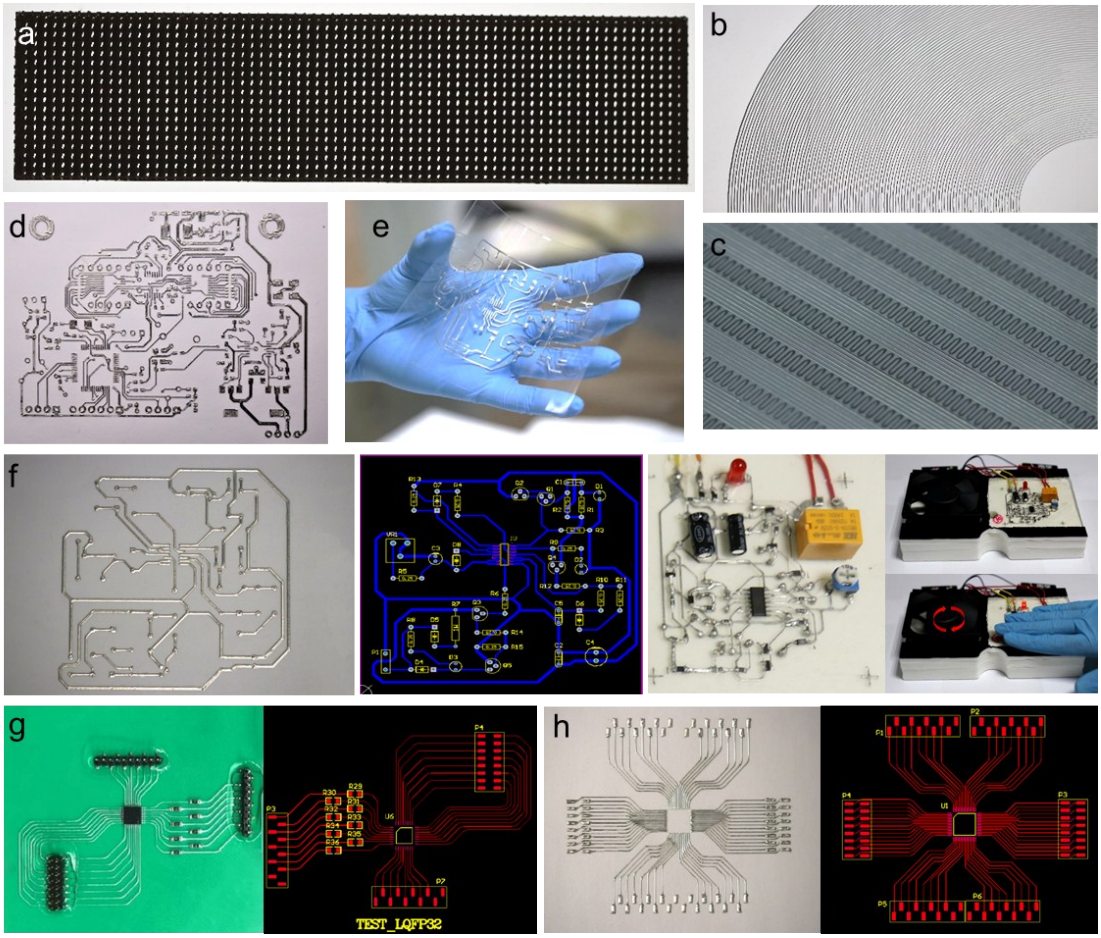

Figure S3. More patterns fabricated by the solidified circuit printing method with low-melting metal. (a) Dot-matrix. (b) Arc curves of different radius. (c) Snake curves. (d) A printed circuit board without electronic components. (e) A bendable circuit board on the PET substrate. (f) A single-layer circuit board for the inductive fan and its PCB design drawing. (g) A solidify circuit board with an LQFP32 chip and its PCB design drawing. (h) The PCB design drawing of the solidify circuit board with an LQFP 64 chip shown in Figure 1e.

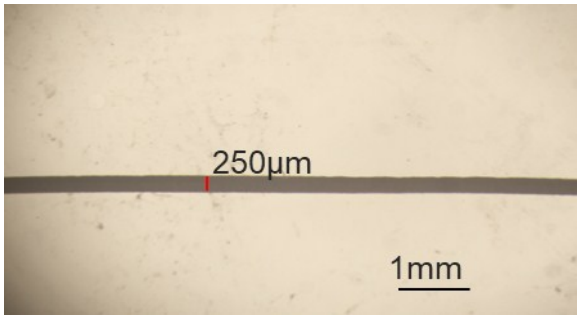

Figure S4. A printed line with a width of 250μm when the print heat runs only once with the slowest speed (1.5mm/s).

As for the linear relationship between the line resistance value and print speed, we have added a detailed discussion in the supplementary information as follows.

"Through the study of the printing process, we can obtain:

$$q_{outlet} = vS_{line} \tag{1}$$

where v is the printing speed, and S_{line} is the cross-sectional area of the printed line. Therefore, at a certain printing speed, S_{line} is proportional to q_{outlet}.

The formula of resistance is

$$R_{line} = \rho L / S_{line} \tag{2}$$

where R_{line} is the resistance value of the printed line with a certain length L, and ρ is the electrical conductivity, which is a constant.

According to formulas (1) ~ (2) we can get:

$$R_{line} = \rho L v / q_{outlet} \tag{3}$$

In the printing process, due to the constant pressure boundary conditions, q_{outlet} is also a fixed value during the printing process, so the resistance value is proportional to the print speed."

As for the nonlinear relationship between the line width and print speed, we have also added a detail discussion in the supplementary information as follows

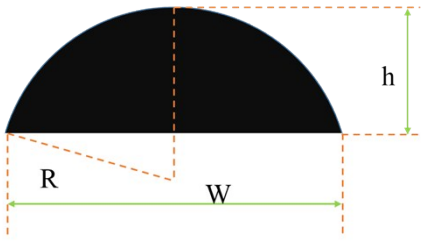

Figure S5. Schematic diagram of the cross-sectional contour of a single print line

The cross-section of a single print is arc-shaped, so the relationship between the width W of the printed line and the cross-sectional area S_{line} is:

$$S_{line} = \pi R^2 * 2\arcsin\left(\frac{W/2}{R}\right) - \frac{W}{2}(R-h) \tag{4}$$

In addition, according to the geometric relationship in Figure S5,

$$R = \frac{\frac{W^2}{4} + h^2}{2h} \tag{5}$$

So

$$S_{line} = \pi\frac{(\frac{W^2}{4} + h^2)^2}{2h^2}\arcsin\left(\frac{hW}{\frac{W^2}{4} + h^2}\right) - \frac{W}{2}\left(\frac{\frac{W^2}{4} + h^2}{2h} - h\right) \tag{6}$$

It can be seen that the relationship between the width of the printed line and the cross-sectional area is very complicated, not a linear relationship.

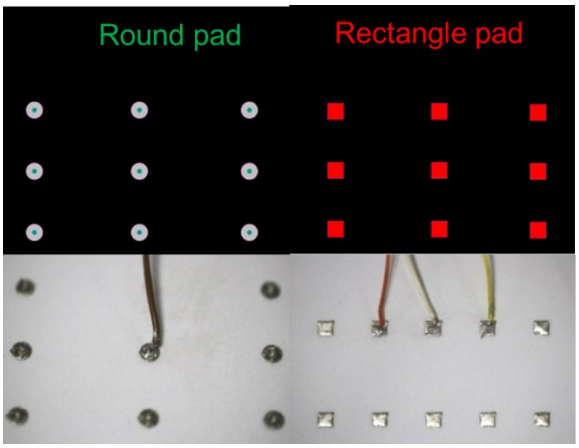

Figure S6. Round pads and rectangle pads detached from the substrate for the adhesion measurement. The upper is the design drawing of the printing pads, and the lowers are the printed round pads and rectangle pads.

To evaluate the effect of the surface oxides on the life of the rolling-ball head, the ink tube was full of BiInSn beads (about 40g for $Bi_{32.5}In_{51}Sn_{16.5}$ beads), and then the printing process continued unless the ink didn't flow down to the substrate. It was found that the printing process stopped until the BiInSn beads in the ink tube were used out. Figure S7 revealed the total length of printed lines, about four hundreds of milliliters. If the BiInSn beads was refilled, the printing process can go on.

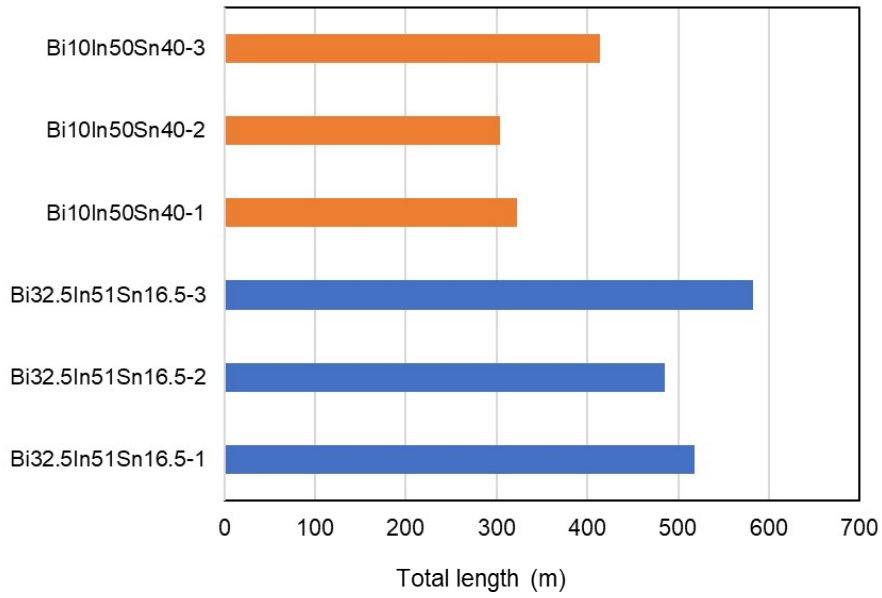

Figure S7. The total length of printed lines.

However, long-term use will still make the rolling-ball head be blocked. We removed the rolling-ball heads from two pen heads that have been in use for a long time. As shown in Figure S8, there are many impurities which have more oxygen element on the surface of the used rolling-ball heads. Therefore, it can be deduced that when the melting ink flows out of the penpoint, part of the surface oxides will attach to the surface of the rolling-ball head and accumulates until the penpoint is blocked.

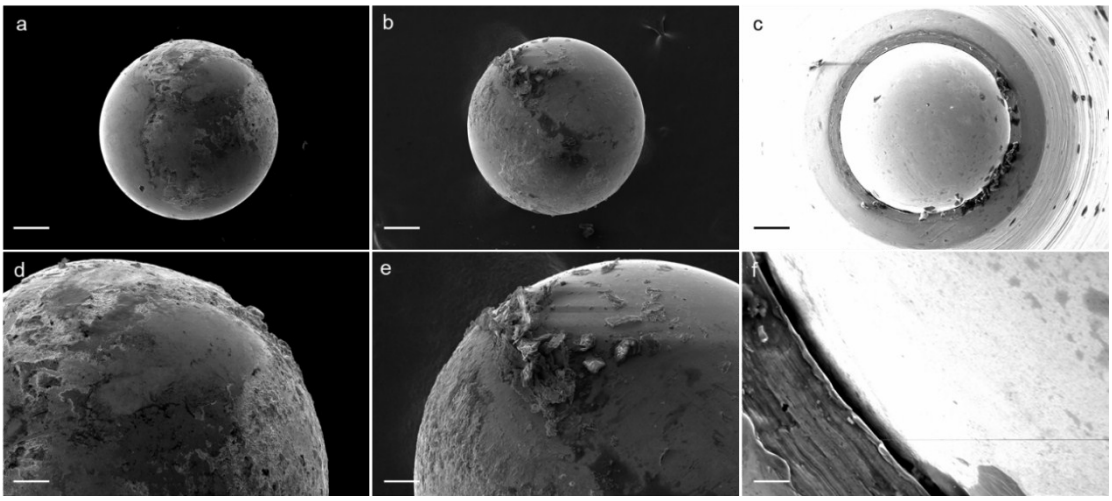

Figure S8. SEM images of the rolling-ball heads. (a) Rolling-ball heads using $Bi_{32.5}In_{51}Sn_{16.5}$ alloy for a long time. (b) Rolling-ball heads using $Bi_{10}In_{50}Sn_{40}$ alloy for a long time. (c) a new one as a control experiment. (d)-(f) are the enlarged images of (a)-(c).

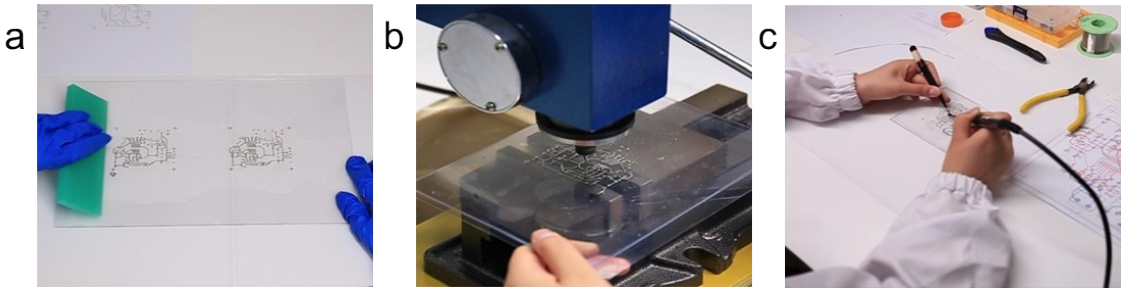

Figure S9. The fabrication process of the double-sided circuit board by the solidified circuit printing method with low-melting metal. (a) Circuit board aligning and bonding. (b) Circuit board punching. (c) Low-temperature welding of the via holes.

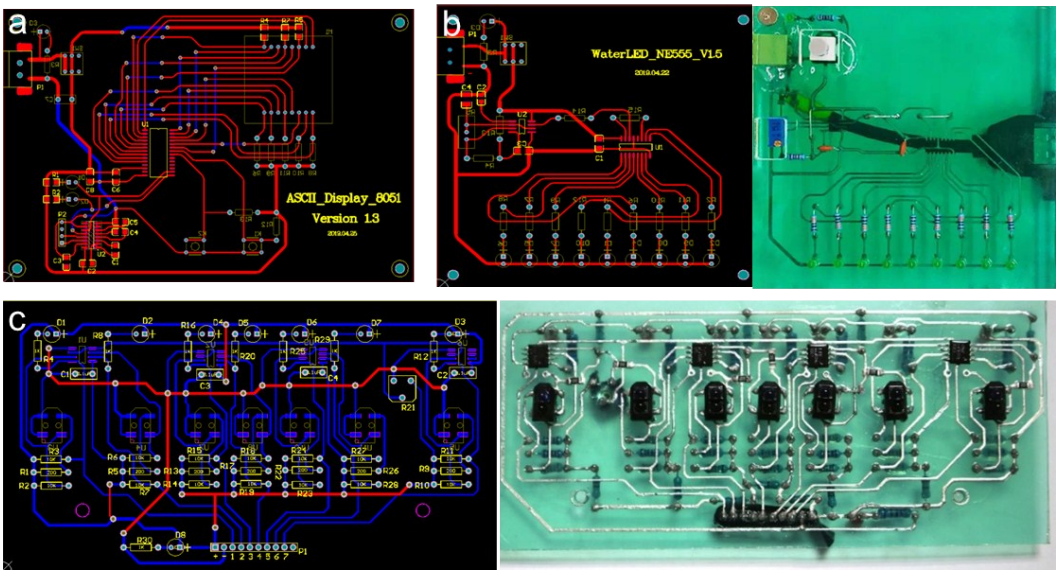

Figure S10. More double-layer circuit boards and their PCB design drawing fabricated by the solidified circuit printing method with low-melting metal. (a) PCB design drawing of the LED digital display circuit based on an 8051 microchip. (b) A double-layer circuit of flowing water light and its PCB design drawing. (c) A double-layer circuit of infrared tracking and its PCB design drawing.

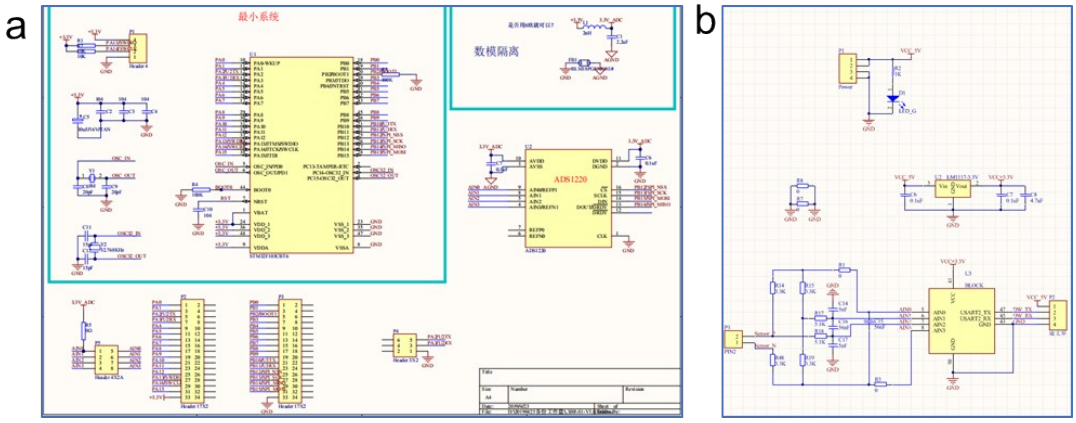

Figure S11. (a) The circuit schematic diagrams of the core board in Figure 6. (b) The circuit schematic diagrams of the BiInSn solidify circuit board in Figure 6.

References

1. Hawkins, R., Reliability Improvements in Commercial/Industrial Grade Integrated Circuit Devices. Manufacturing Technology IEEE Transactions on, 1976. 5(3): p. 58-61.
2. Clark, D.T., et al., High Temperature Silicon Carbide CMOS Integrated Circuits. Materials science forum, 2011. 679-680: p. p.726-729.
3. Forbes, L. and P.A. Farrar, Operation and design of integrated circuits at constrained temperature ranges in accordance with bit error rates. 2007.
4. Mccluskey, P., et al. Reliability of commercial plastic encapsulated microelectronics attemperatures from 125°C to 300°C. in IEEE Aerospace Conference. 2000.
5. Burke, A., Gamma and temperature hardened pharmaceutical devices. 2014, US.

Table S1 The melting points of other low-melting alloys composed of Bi, In, Sn and Zn (less than 100 ℃)

Bi	**In**	**Sn**	**Zn**	**Melting point（^{o}C）**	**Bi**	**In**	**Sn**	**Zn**	**Melting point（^{o}C）**
33.7	66.3			72 E	47.4	52.2		0.4	85.78
57.2	24.8	18.6		77.5	32.7	66.9		0.4	67.86
57	26	17		79 E	32.7	66.9		0.5	67.77
54.3	27.9	17.7		75.22	53.5	28.0	18.1	0.4	74.12
54	29.7	16.3		81 E	33.1	64.1	2.4	0.5	67.53
43.2	39.3	17.5		70.38	40.6	41.3	17.6	0.5	66.86
36.1	50.2	13.7		60.57	36.1	48.3	15.6	0.3	58.85

31.6	48.8	19.6		59	35.0	50.2	14.4	0.4	58.45
36.1	48.3	15.5		58.89	35.3	48.3	15.9	0.4	57.45
36.1	48.3	15.6		58.98	35.0	48.6	15.9	0.4	57.23
48.8	50.8		0.4	86.81					

Table S2. Electrical conductivity values of various BiInSn alloys

BiInSn alloys	Electrical conductivity (10^6 S/m)			
	Test 1	Test 2	Test 3	Mean±SD
$Bi_{32.5}In_{51}Sn_{16.5}$	2.48	2.47	2.43	2.46±0.026
$Bi_{54}In_{28}Sn_{18}$	1.34	1.37	1.35	1.35±0.015
$Bi_{10}In_{50}Sn_{40}$	3.87	3.86	3.85	3.86±0.01

Supplementary Movie description:

Movie S1. The printing process of solidified circuit direct printing method with low melting point metal.

Movie S2. Display of the printed lines by the solidified circuit printing method.

Movie S3. Printed single-sided circuit for an inductive fan.

Movie S4. Printed double-sided circuit for a light control switch.

Movie S5. Combination of the solid circuit and packaged liquid circuit fabricated by the solidified circuit direct printing method.